

# Adsorption of CO on Pt<sub>3</sub>, Pd<sub>3</sub>, Pd Doped Pt<sub>2</sub> and Pt Doped Pd<sub>3</sub> Clusters: A Density Functional Study

<sup>1</sup>Md. Asaduzzaman, <sup>1</sup>Apu Kumar Ghosh and <sup>1</sup>Md. Khorshed Alam

<sup>1</sup>Department of Physics, University of Barishal, Barishal-8254.

\*khorshed\_du@yahoo.com

**Abstract:** The adsorption of carbon monoxide (CO) on nanoscale clusters is a topic of significant interest for catalytic and gas sensing applications. Quantum mechanical density functional theory (DFT) and molecular mechanics (MM) simulations were employed to investigate the interactions between carbon monoxide (CO) and Pt<sub>3</sub>, Pd<sub>3</sub>, Pd-doped Pt<sub>2</sub>, and Pt-doped Pd<sub>2</sub> clusters. The aim of this research was to study the adsorption of CO on these clusters and understand the resulting changes in geometric and electronic properties. Our methodology involved performing DFT calculations to determine the adsorption energies, examining the bond lengths and binding energies of CO, and analyzing the electronic properties of the clusters. The key findings of our study revealed favorable adsorption of CO on all clusters, with notable modifications in bond lengths and binding energies. Among the clusters, Pt-doped Pd<sub>2</sub> exhibited the highest adsorption energy, suggesting its potential as an efficient catalyst for CO removal and oxidation. Furthermore, the electronic properties of the clusters provided insights into their suitability for CO sensing applications. Overall, our research contributes to the understanding of CO adsorption behavior on nanoscale clusters and highlights the significance of Pt-doped Pd<sub>2</sub> in CO-related applications, such as catalysis and gas sensing.

**Keywords:** *Carbon monoxide (CO), Nanoscale clusters, Adsorption, Density functional theory (DFT), Catalysis*

## 1. Introduction:

Adsorption is a fundamental process that occurs at the interface between different phases and plays a vital role in numerous physical, chemical, and biological processes [1]. Understanding adsorption phenomena is essential for various applications, including separation techniques and industrial-scale processes [1]. While solid-gas and solid-liquid interfaces have received significant attention in industrial adsorption processes, all types of interfaces are relevant in laboratory separation techniques [1]. The term "fluid" is commonly used to refer to gases or liquids in contact with solid surfaces [1].

Catalytic oxidation of carbon monoxide (CO) is an extensively studied reaction due to its environmental and energy-related significance. Transition metals, such as palladium, platinum, and rhodium, have

demonstrated exceptional catalytic activity in enhancing the CO oxidation process [2], [3]. Palladium and platinum catalysts, in particular, are widely used in commercial three-way catalysts to reduce automotive emissions by converting CO to CO<sub>2</sub> [4], [5]. The understanding of CO oxidation is not limited to the strength of the bond between oxygen and the metal surface, but also involves the dissociation of O<sub>2</sub> and the diffusion of adsorbates on the surface [6]. Co-adsorption properties of CO and oxygen are crucial for studying catalytic CO oxidation [4], [7], [16]–[18], [8]–[15].

Prior research has provided evidence of size effects in CO oxidation reactions on single-crystal surfaces and supported clusters, highlighting the intrinsic size dependence of palladium [18], [19]. Experimental studies have shed light on the molecular understanding of size effects for CO oxidation by palladium, with scanning tunneling microscopy revealing enhanced reactivity of adsorbed oxygen due to co-adsorption of CO [10]–[12]. Investigation of the reactivity of different Pd-O species has shown a decrease in reactivity with increasing oxidation state [13]. Furthermore, studies on supported Pd clusters have reported the oxidation of CO using various experimental and theoretical techniques [13], [15]–[17].

Carbon monoxide (CO) chemistry is of great importance due to its toxicity and presence as a subproduct of automobile exhausts. CO conversion to non-toxic CO<sub>2</sub> is desirable, and in the context of fuel cells, CO poisoning is a major catalyst deactivation mechanism [20], [21]. The interaction between CO and various metallic systems, such as metal surfaces, nanoparticles, and single atoms, has been extensively investigated in terms of adsorption energy and CO molecule activation [22]–[24]. Small cluster model systems have proven to be valuable in understanding the microscopic details of this interaction [25], [26].

Pt<sub>3</sub> clusters, composed of three platinum atoms, exhibit unique properties that make them highly effective catalysts. Their high catalytic activity, attributed to a high surface area and distinctive electronic structure, has been observed in various chemical reactions, including the oxygen reduction reaction (ORR) in fuel cells and the hydrogenation of unsaturated hydrocarbons [2], [3]. Pd<sub>3</sub> clusters, consisting of three palladium atoms, also possess a high surface area and serve as efficient catalysts in the hydrogenation of unsaturated hydrocarbons [2], [3]. Pt-doped Pd<sub>2</sub> clusters and Pd-doped Pt<sub>2</sub> clusters

show enhanced catalytic activity and modified electronic structures, making them promising candidates for various reactions, including the hydrogenation of unsaturated hydrocarbons [2], [3]. This study aims to investigate the adsorption of CO on Pt<sub>3</sub>, Pd<sub>3</sub>, Pd doped Pt<sub>2</sub>, and Pt doped Pd<sub>3</sub> clusters using density functional theory (DFT) calculations. By examining the CO adsorption properties of these clusters, we seek to gain insights into their catalytic behavior and provide a deeper understanding of the CO oxidation process. The findings of this study may contribute to the development of more efficient catalytic systems and advance our knowledge in the field of CO adsorption on metal clusters.

## 2. Background Theory:

### 2.1. Background Theory and Principles of DFT:

Density functional theory (DFT) is a powerful tool in bioinorganic chemistry, condensed matter physics, materials science and superconductivity for modeling structures, properties, and processes related to photosynthesis. It replaces the many-body wavefunction with the electronic density as the basic quantity, making it computationally efficient. DFT is based on the principles established by Hohenberg and Kohn, which state that the ground-state electron density uniquely determines the electronic wavefunction and energy of the system [27]. The Kohn-Sham (KS) approach, a variant of the Hartree-Fock method, is commonly used in DFT to construct a noninteracting system with the same density as the original problem. Various approximations, such as local-density approximation (LDA), generalized gradient approximation (GGA), and hybrid functionals, are used to approximate the exchange-correlation functional, which is the main challenge in DFT calculations [28]. While DFT has limitations and uncertainties, it offers a close connection between theory and experiment and continues to be a valuable tool in bioinorganic chemistry research.

### 2.2. Properties and Applications of DFT:

DFT has found numerous applications in bioinorganic chemistry, offering insights into molecular properties, reaction mechanisms, vibrational frequencies, optical spectra, and exchange couplings. It provides reliable predictions for molecular geometries, with optimized structures closely matching experimental data [29]. Energetic predictions and the study of reaction mechanisms are also important applications of DFT, although the accuracy can vary, especially for complex systems. Vibrational frequencies can be calculated with reasonable accuracy, particularly for strong metal-ligand bonds [30]. Optical spectra predictions using time-dependent DFT (TD-DFT) calculations can be useful but require caution and validation against experimental data [31]. DFT also plays a role in determining exchange coupling constants in systems with interacting magnetic ions, although careful

analysis and comparison with experimental observations are necessary [32]. While DFT has shown success in bioinorganic chemistry, it is important to consider its limitations and to continuously improve its accuracy and applicability in future developments.

## 3. Methodology:

In this study, computational techniques based on density functional theory (DFT) were employed to investigate the adsorption energies of CO on Pt<sub>3</sub>, Pd<sub>3</sub>, Pd-doped Pt<sub>2</sub>, and Pt-doped Pd<sub>2</sub> clusters. The calculations were performed using the DMol<sup>3</sup> software package (DMol<sup>3</sup>) developed by Materials Studio [33].

To begin, the initial structures of CO, Pt<sub>3</sub>, Pd<sub>3</sub>, Pd-doped Pt<sub>2</sub>, and Pt-doped Pt<sub>2</sub> clusters were constructed using the Material Studio software [33]. The geometries of these structures were then optimized within the Material Studio environment to obtain stable and relaxed configurations.

Self-consistent field (SCF) procedures were performed with a convergence criterion of  $1 \times 10^{-5}$  Ha for the total energy and  $10^{-5}$  Ha for the electron density, ensuring accurate results.

For the basis set, we utilized the double-numerical with polarization (DNP) basis set available in DMol<sup>3</sup> [33]. This basis set consists of a double set of numerically tabulated basis functions, which enhances the accuracy of the calculations. The DNP basis set includes higher angular momentum valence polarization functions and core polarization functions, making it more complete compared to linearly independent Gaussian function sets. The exchange-correlation functional chosen for our calculations was the generalized gradient approximation (GGA), specifically the B3LYP functional. The B3LYP functional combines the exchange functional developed by Becke [34] with the gradient-corrected correlation functional of Lee et al. [35]. Additionally, spin-polarized calculations were performed using the spin-interpolation method of Vosko et al. [36].

To locate the transition state structures, the transition state search option available in DMol<sup>3</sup> [33] was utilized. The search for transition states was based on the linear (LST) and quadratic synchronous transit (QST) methods proposed by Halgren and Lipscomb [37]. In the LST approach, a series of single point energy calculations were performed on a set of linearly interpolated structures between the reactant and product configurations. The maximum energy structure along this path provided an initial estimate of the transition state structure. A single refinement step in an orthogonal direction to the LST path was then performed, resulting in an intermediate structure that defined the QST pathway. This procedure yielded a further refined estimate of the transition state geometry, allowing

for rapid and accurate location of the transition states.

Finally, the adsorption energies ( $E_{\text{ads}}$ ) of CO on Pt<sub>3</sub>, Pd<sub>3</sub>, Pd-doped Pt<sub>2</sub>, and Pt-doped Pd<sub>2</sub> clusters were calculated using the following equations:

$$E_{\text{ads}}(\text{Pt}_3) = E(\text{Pt}_3 - \text{CO}) - (E_{\text{Pt}_3} + E_{\text{CO}}) \dots \dots (1)$$

$$E_{\text{ads}}(\text{Pd}_3) = E(\text{Pd}_3 - \text{CO}) - (E_{\text{Pd}_3} + E_{\text{CO}}) \dots \dots (2)$$

$$E_{\text{ads}}(\text{Pd} - \text{Pt}_2) = E(\text{Pd} - \text{Pt}_2 - \text{CO}) - (E_{\text{Pd-Pt}_2} + E_{\text{CO}}) \dots \dots (3)$$

$$E_{\text{ads}}(\text{Pt} - \text{Pd}_2) = E(\text{Pt} - \text{Pd}_2 - \text{CO}) - (E_{\text{Pt-Pd}_2} + E_{\text{CO}}) \dots \dots (4)$$

In these equations,  $E(\text{Pt}_3\text{-CO})$ ,  $E(\text{Pd}_3\text{-CO})$ ,  $E(\text{Pd-Pt}_2\text{-CO})$ , and  $E(\text{Pt-Pd}_2\text{-CO})$  represent the total energies of the respective CO adsorbed clusters, while  $E_{\text{Pt}_3}$ ,  $E_{\text{Pd}_3}$ ,  $E_{\text{Pd-Pt}_2}$ , and  $E_{\text{Pt-Pd}_2}$  denote the total energies of the unadsorbed clusters.  $E_{\text{CO}}$  corresponds to the total energy of an isolated CO molecule.

By employing the above computational techniques and calculations, we aimed to gain insights into the

adsorption energies of CO on different clusters and their implications for catalytic processes.

## 4. Results and Discussion:

### 4.1. Adsorption Energies and Structures of CO on Clusters:

We investigated the adsorption energies of CO on Pt<sub>3</sub>, Pd<sub>3</sub>, Pd-doped Pt<sub>2</sub>, and Pt-doped Pd<sub>2</sub> clusters using computational techniques based on DFT. The calculated adsorption energies and structures for CO on each cluster are summarized in Table-1.

### 4.2. Cluster Properties and Electronic Structure:

Table-1 (see below) presents the total energy, total binding energy, HOMO and LUMO energies, bandgap, and dipole moment of CO, Pt<sub>3</sub>, Pd<sub>3</sub>, Pd-doped Pt<sub>2</sub>, and Pt-doped Pd<sub>2</sub> clusters. These properties provide insights into the stability, adsorption strength, electronic structure, and polarity of each system.

Table 1: Total energy, Total binding energy, HOMO and LUMO energy, Band gap and Dipole moment of CO, Pt<sub>3</sub>, Pd<sub>3</sub>, Pd doped Pt<sub>2</sub>, Pt doped Pd<sub>2</sub>.

Molecule	$E_{\text{HOMO}}$ (eV)	$E_{\text{LUMO}}$ (eV)	Bandgap $\Delta E$ (eV)
CO	-10.35	-0.90	-9.45
Pt <sub>3</sub>	-5.39	-4.07	-1.32
Pd <sub>3</sub>	-4.09	1.31	-2.78
Pd doped Pt <sub>2</sub>	-5.21	-4.18	-1.03
Pt doped Pd <sub>2</sub>	-5.15	-4.13	-1.02

### 4.3. Electronic Properties and Reactivity:

The HOMO and LUMO energies of CO and the clusters were determined, providing insights into the electron distribution, reactivity, and energy levels of the systems. The bandgap values indicate the energy range for electronic transitions. The dipole moments characterize the polarity and charge distribution of each cluster.

### 4.4. Complex Structures of CO and Clusters:

Figure 1(a) shows the structure of Pt<sub>3</sub> cluster, consisting of three bonded platinum atoms. Figure

1(b) depicts the structure of Pd<sub>3</sub> cluster, composed of three bonded palladium atoms. Figure 1(c) displays the structure of the Pd-doped Pt<sub>2</sub> cluster, with two platinum and one palladium atom forming the cluster. Figure 1(d) illustrates the structure of the Pt-doped Pd<sub>2</sub> cluster, consisting of one platinum and two palladium atoms. Figure 1(e) presents the structure of carbon monoxide (CO), with a triple bond between carbon and oxygen.

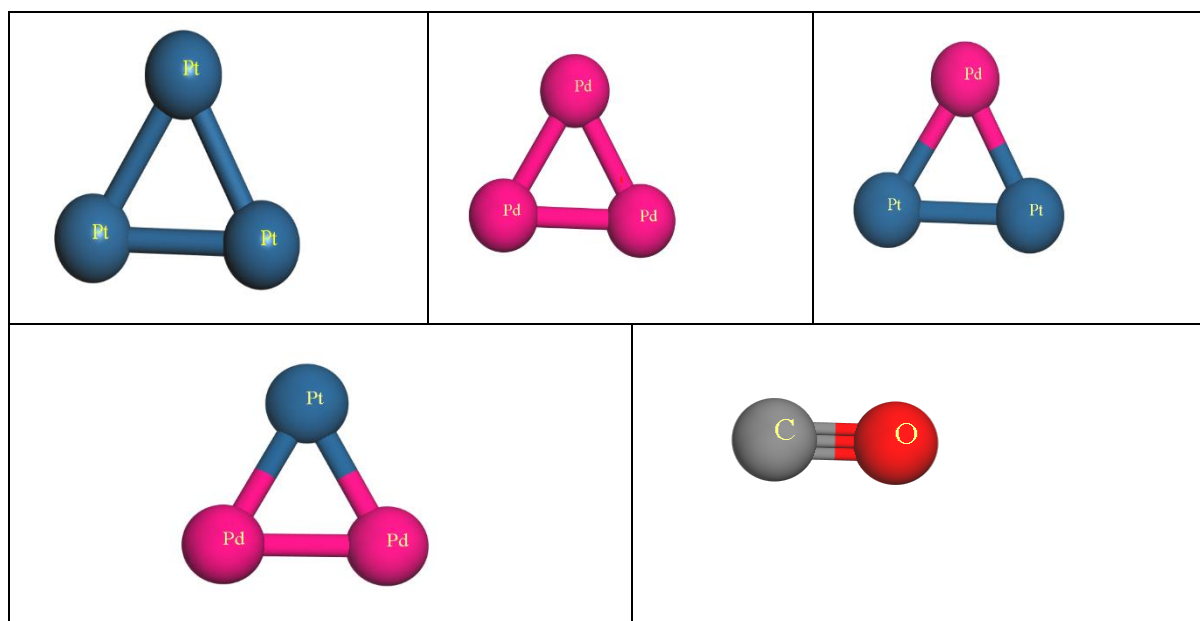


Fig. 1: (a) Pt<sub>3</sub> Cluster, (b) Pd<sub>3</sub> Cluster, (c) Pd doped Pt<sub>2</sub> Cluster, (d) Pt doped Pd<sub>2</sub>, and (e) Carbon Monoxide (CO).

#### 4.5. Properties of CO-Cluster Complexes:

The total energies, binding energies, HOMO and LUMO energies, and dipole moments of the Pt<sub>3</sub>-CO, Pd<sub>3</sub>-CO, Pd-doped Pt<sub>2</sub>-CO, and Pt-doped Pd<sub>2</sub>-CO complexes are provided in Table-2 (see below). The dipole moments reflect the changes in polarity upon CO adsorption. The calculated adsorption energy has good agreement with previous report [38].

Table 2: Total energy, HOMO-LUMO energy, Bandgap, Dipole moment & Adsorption energy of Pt<sub>3</sub>-CO, Pd<sub>3</sub>-CO, Pd-Pt<sub>2</sub>-CO, Pt-Pd<sub>2</sub>-CO.

Molecule	Total energy (eV)	E <sub>(HOMO)</sub> (eV)	E <sub>(LUMO)</sub> (eV)	Bandgap ΔE (eV)	E <sub>ads</sub> (eV)
CO	-3261.29	-10.347	-0.90	-9.45	-0.8641
Pt <sub>3</sub>	-1431154.32	-5.387	-4.07	-1.32	
Pt <sub>3</sub> -CO	-1434416.48	-5.485	-4.06	-1.43	
CO	-3261.29	-10.347	-0.90	-9.45	-0.898
Pd <sub>3</sub>	-410030.69	-4.092	-1.31	-2.78	
Pd <sub>3</sub> -CO	-413292.88	-5.435	-4.08	-1.35	
CO	-3261.29	-10.347	-0.90	-9.45	-0.885
Pd-Pt <sub>2</sub>	-1090779.82	-5.209	-4.18	-1.03	
Pd-Pt <sub>2</sub> -CO	-1094042.01	-5.634	-4.24	1.39	
CO	-3261.29	-10.347	-0.90	-9.45	-1.278
Pt-Pd <sub>2</sub>	-750405.26	-5.149	-4.13	-1.02	
Pt-Pd <sub>2</sub> -CO	-753667.83	-5.582	-4.24	1.34	

#### 4.6. OMO and LUMO Energies of CO-Cluster Complexes:

Figures 2 and 3 depict the HOMO and LUMO orbitals of CO, Pt<sub>3</sub>, Pd<sub>3</sub>, Pd-doped Pt<sub>2</sub>, and Pt-doped Pd<sub>2</sub> clusters, as well as the Pt<sub>3</sub>-CO, Pd<sub>3</sub>-CO, Pd-

doped Pt<sub>2</sub>-CO, and Pt-doped Pd<sub>2</sub>-CO complexes. These figures highlight the electronic properties, reactivity, and electron distribution within the systems.

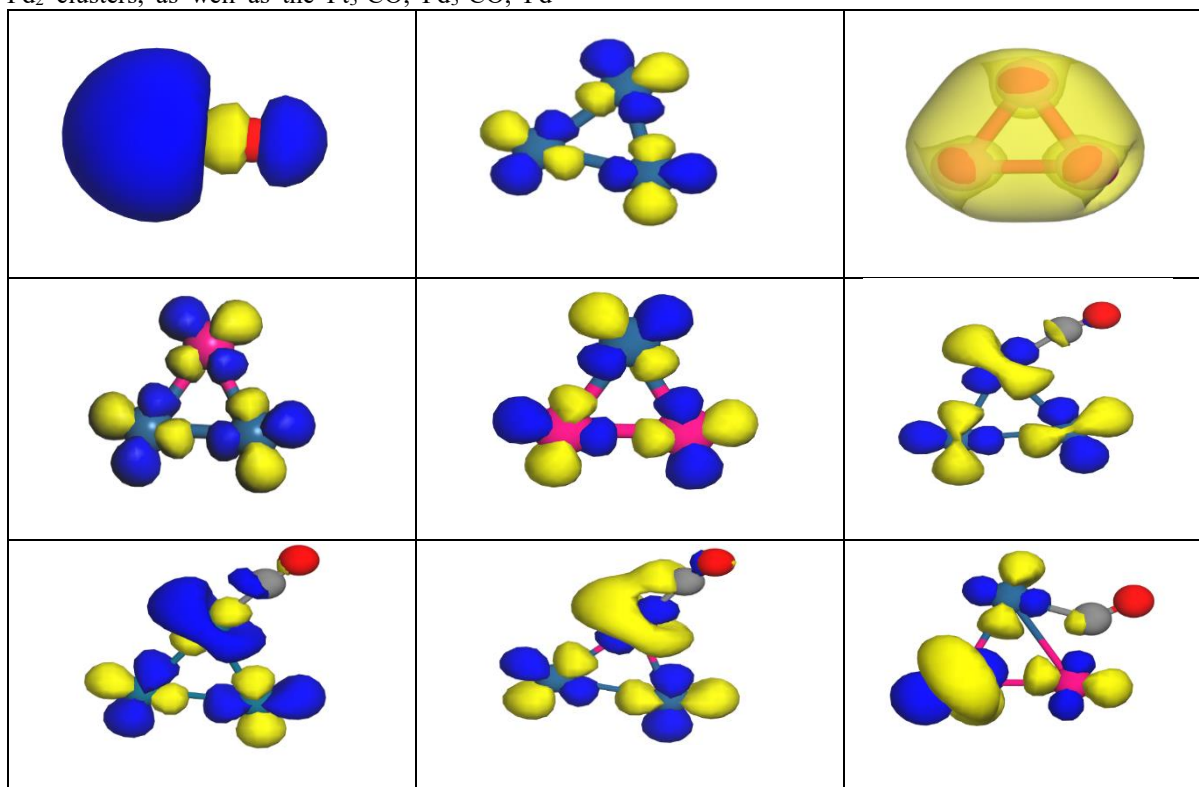


Fig. 2: HOMO orbitals of (a) CO, (b) Pt<sub>3</sub>, (c) Pd<sub>3</sub>, (d) Pd doped Pt<sub>2</sub>, (e) Pt doped Pd<sub>2</sub> clusters, as well as (f) Pt<sub>3</sub>-CO, (g) Pd<sub>3</sub>-CO, (i) Pd-doped Pt<sub>2</sub>-CO, and (j) Pt-doped Pd<sub>2</sub>-CO complexes.

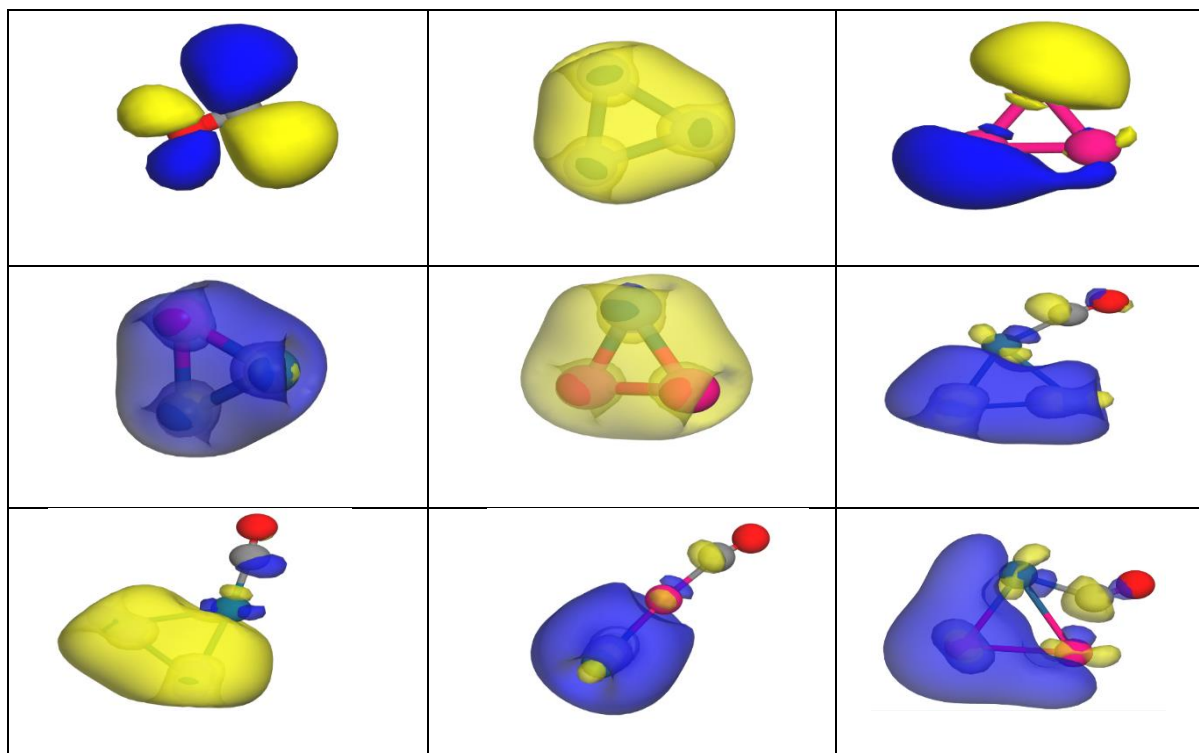


Fig. 3: LUMO orbitals of (a) CO, (b) Pt<sub>3</sub>, (c) Pd<sub>3</sub>, (d) Pd doped Pt<sub>2</sub>, (e) Pt doped Pd<sub>2</sub> clusters, as well as (f) Pt<sub>3</sub>-CO, (g) Pd<sub>3</sub>-CO, (i) Pd-doped Pt<sub>2</sub>-CO, and (j) Pt-doped Pd<sub>2</sub>-CO complexes.

#### 4.7. Discussion of Differences and Implications:

The results indicate significant differences in the adsorption energies and structures of CO on Pt<sub>3</sub>, Pd<sub>3</sub>, Pd-doped Pt<sub>2</sub>, and Pt-doped Pd<sub>2</sub> clusters. These differences can be attributed to the composition and arrangement of metal atoms, which influence the adsorption behavior of CO. The dipole moments and HOMO-LUMO energies provide insights into the electronic interactions between CO and the clusters.

#### 4.8. Limitations and Considerations:

It is important to acknowledge the limitations of this study, including the specific computational

techniques used and the chosen model systems. The results may be subject to uncertainties and may not fully capture the complexity of real catalytic processes. In conclusion, this study provides valuable insights into the adsorption energies of CO on Pt<sub>3</sub>, Pd<sub>3</sub>, Pd-doped Pt<sub>2</sub>, and Pt-doped Pd<sub>2</sub> clusters. The findings contribute to the understanding of catalytic processes involving CO adsorption and highlight the potential applications of these clusters in various fields, such as catalysis and materials science.

### 5. Conclusion:

Our study utilizing density functional theory calculations reveals that CO adsorption on Pt<sub>3</sub>, Pd<sub>3</sub>, Pd-doped Pt<sub>2</sub>, and Pt-doped Pd<sub>2</sub> clusters is favorable, resulting in changes in bond length and binding energy (Table-1). Pt-Pd<sub>2</sub> cluster exhibits the highest adsorption energy, making it a promising candidate for CO sensing and catalyzing CO oxidation. This cluster can potentially replace pure platinum and palladium in applications such as CO removal in vehicles. Additionally, all clusters show potential for CO sensing (Figures 2 and 3). These findings are in

agreement with previous studies on CO adsorption on metal clusters [23], [32], [39]–[41]. Overall, these results contribute to the development of efficient materials for CO adsorption and sensing, with implications in catalysis, materials science, and environmental engineering. Further experimental investigations are needed to validate our computational results and explore the practical applications of Pt-Pd<sub>2</sub> cluster in CO removal and sensing. The understanding gained from this study can guide future research in the design and optimization of cluster-based catalysts for CO-related applications.

### 6. References:

- [1]. W. J. Weber, "Adsorption processes," *Pure Appl. Chem.*, vol. 37, no. 3, pp. 375–392, 1974, doi: 10.1351/pac197437030375.
- [2]. S. Royer and D. Duprez, "Catalytic Oxidation of Carbon Monoxide over Transition Metal Oxides," *ChemCatChem*, vol. 3, no. 1, pp. 24–65, 2011, doi: 10.1002/cctc.201000378.
- [3]. A. K. Santra and D. W. Goodman, "Catalytic oxidation of CO by platinum group metals: From ultrahigh vacuum to elevated pressures," *Electrochim. Acta*, vol. 47, no. 22–23, pp. 3595–3609, 2002, doi: 10.1016/S0013-4686(02)00330-4.
- [4]. S. Nandi *et al.*, "Relationship between design strategies of commercial three-way monolithic catalysts and their performances in realistic conditions," *Catal. Today*, vol. 384–386, pp. 122–132, 2022, doi: 10.1016/j.cattod.2021.05.005.
- [5]. K. V. T. R. R. P. S. V. A. P. Nilay Jani, "IRJET- Development and Performance Analysis of Zn based Catalytic Converter," *Irjet*, vol. 8, no. 4, pp. 2932–2942, 2021, doi: 10.9790/1684-1705042833.
- [6]. M. M. Montemore, M. A. Van Spronsen, R. J. Madix, and C. M. Friend, "O<sub>2</sub> Activation by Metal Surfaces: Implications for Bonding and Reactivity on Heterogeneous Catalysts," *Chem. Rev.*, vol. 118, no. 5, pp. 2816–2862, 2018, doi: 10.1021/acs.chemrev.7b00217.
- [7]. B. Demirdjian, I. Ozerov, F. Bedu, A. Ranguis, and C. R. Henry, "CO and O<sub>2</sub> Adsorption and CO Oxidation on Pt Nanoparticles by Indirect Nanoplasmonic Sensing," *ACS Omega*, vol. 6, no. 20, pp. 13398–13405, 2021, doi: 10.1021/acsomega.1c01487.
- [8]. T. Bunluesin, R. J. Gorte, and G. W. Graham, "CO oxidation for the characterization of reducibility in oxygen storage components of three-way automotive catalysts," *Appl. Catal. B Environ.*, vol. 14, no. 1–2, pp. 105–115, 1997, doi: 10.1016/S0926-3373(97)00016-7.
- [9]. R. M. Al Soubaihi, K. M. Saoud, and J. Dutta, "Critical review of low-temperature CO oxidation and hysteresis phenomenon on heterogeneous catalysts," *Catalysts*, vol. 8, no. 12, 2018, doi: 10.3390/catal8120660.
- [10]. V. A. Nasluzov, E. A. Ivanova-Shor, A. M. Shor, S. S. Laletina, and K. M. Neyman, "Adsorption and oxidation of CO on ceria nanoparticles exposing single-atom Pd and Ag: A DFT modelling," *Materials (Basel)*, vol. 14, no. 22, pp. 17–20, 2021, doi: 10.3390/ma14226888.
- [11]. N. Yigit, A. Genest, S. Terloev, J. Moller, and G. Rupprechter, "Active sites and deactivation of room temperature CO oxidation on Co<sub>3</sub>O<sub>4</sub> catalysts: combined experimental and computational investigations," *J. Phys. Condens. Matter*, vol. 34, no. 35, 2022, doi: 10.1088/1361-648X/ac718b.
- [12]. X. Wang and T. Bürgi, "Influence of the Time Scale on the Reaction Mechanism of CO Oxidation over a Au/TiO<sub>2</sub> Catalyst," *Angew. Chemie - Int. Ed.*, vol. 202300146, pp. 1–9, 2023, doi: 10.1002/anie.202300146.
- [13]. Y. Yi *et al.*, "Low temperature CO oxidation catalysed by flower-like Ni-Co-O: How physicochemical properties influence catalytic performance," *RSC Adv.*, vol. 8, no. 13, pp. 7110–7122, 2018, doi: 10.1039/c7ra12635b.
- [14]. L. Wang, S. Deo, K. Dooley, M. J. Janik, and R. M. Rioux, "Influence of metal nuclearity and physicochemical properties of ceria on the oxidation of carbon monoxide," *Chinese J. Catal.*, vol. 41, no. 6, pp. 951–962, 2020, doi: 10.1016/S1872-2067(20)63557-4.
- [15]. J. Zhang *et al.*, "Wet-Chemistry Strong Metal-Support Interactions in Titania-Supported Au Catalysts," *J. Am. Chem. Soc.*, vol. 141, no. 7, pp. 2975–2983, 2019, doi:

10.1021/jacs.8b10864.

- [16]. A. M. Gänzler, M. Casapu, D. E. Doronkin, F. Maurer, and P. Lott, "The Pt-CeO<sub>2</sub> interface as key for low temperature CO oxidation identified by spatially resolved structure-activity relationships," *Semant. Sch.*, pp. 1–9, 2019.
- [17]. H. J. Freund, G. Meijer, M. Scheffler, R. Schlögl, and M. Wolf, "CO oxidation as a prototypical reaction for heterogeneous processes," *Angew. Chemie - Int. Ed.*, vol. 50, no. 43, pp. 10064–10094, 2011, doi: 10.1002/anie.201101378.
- [18]. O. H. Laguna, L. F. Bobadilla, W. Y. Hernández, and M. A. Centeno, "LOW TEMPERATURE CO OXIDATION," in *Perovskites and related mixed oxides*, pp. 1–31.
- [19]. M. Mahapatra, R. A. Gutiérrez, J. Kang, N. Rui, and R. Hamlyn, "The Behavior of Inverse Oxide / Metal Catalysts : CO Oxidation and Water- gas Shift Reactions over ZnO / Cu ( 111 ) Surfaces," no. 111.
- [20]. I. Three, "Chapter 5 Heterogeneous catalysis," pp. 209–287, 1999, doi: 10.1016/s0167-2991(99)80008-1.
- [21]. M. Nizio, M. Nizio, C. Université, C. Simeon, and C. Patrick, "Plasma catalytic process for CO<sub>2</sub> methanation To cite this version : HAL Id : tel-01612734 Université Pierre et Marie Curie Plasma Catalytic Process for CO<sub>2</sub> Methanation," 2017.
- [22]. D. Wu, D. Han, W. Zhou, S. Streiff, A. Y. Khodakov, and V. V. Ordomsky, "Surface modification of metallic catalysts for the design of selective processes," *Catal. Rev. - Sci. Eng.*, 2022, doi: 10.1080/01614940.2022.2079809.
- [23]. J. Hulva *et al.*, "Unraveling CO adsorption on model single-atom catalysts," *Science (80-. )*, vol. 371, no. 6527, pp. 375–379, 2021, doi: 10.1126/science.abe5757.
- [24]. A. Crampton *et al.*, "Assessing the concept of structure sensitivity or insensitivity for sub-nanometer catalyst materials," *Surf. Sci.*, vol. 652, pp. 7–19, 2016, doi: 10.1016/j.susc.2016.02.006.
- [25]. M. Freer, H. Horiuchi, Y. Kanada-En'Yo, D. Lee, and U. G. Meißner, "Microscopic clustering in light nuclei," *Rev. Mod. Phys.*, vol. 90, no. 3, 2018, doi: 10.1103/RevModPhys.90.035004.
- [26]. D. Bazin *et al.*, "Perspectives on Few-Body Cluster Structures in Exotic Nuclei," *Few-Body Syst.*, vol. 64, no. 2, 2023, doi: 10.1007/s00601-023-01794-0.
- [27]. D. Zhou, "An Introduction of Density Functional Theory and its Application," *Physics.Drexel.Edu*, 2007, [Online]. Available: [http://www.physics.drexel.edu/~bob/Term\\_Reports/Zhou\\_Di\\_4.pdf](http://www.physics.drexel.edu/~bob/Term_Reports/Zhou_Di_4.pdf)
- [28]. M. Freyss and C. De Cadarache, "Chapter 12. Density functional theory," pp. 225–235, 2015.
- [29]. J. Autschbach, "Density functional theory applied to calculating optical and spectroscopic properties of metal complexes: NMR and optical activity," *Coord. Chem. Rev.*, vol. 251, no. 13-14 SPEC. ISS., pp. 1796–1821, 2007, doi: 10.1016/j.ccr.2007.02.012.
- [30]. M. Chen, P. Serna, J. Lu, B. C. Gates, and D. A. Dixon, "Molecular models of site-isolated cobalt, rhodium, and iridium catalysts supported on zeolites: Ligand bond dissociation energies," *Comput. Theor. Chem.*, vol. 1074, pp. 58–72, 2015, doi: 10.1016/j.comptc.2015.09.004.
- [31]. D. Escudero, A. D. Laurent, and D. Jacquemin, "Time-dependent density functional theory: A tool to explore excited states," *Handb. Comput. Chem.*, pp. 927–961, 2017, doi: 10.1007/978-3-319-27282-5\_43.
- [32]. G. Singh, S. Gamboa, M. Orio, D. A. Pantazis, and M. Roemelt, "Magnetic exchange coupling in Cu dimers studied with modern multireference methods and broken-symmetry coupled cluster theory," *Theor. Chem. Acc.*, vol. 140, no. 10, pp. 1–15, 2021, doi: 10.1007/s00214-021-02830-0.
- [33]. M. Studio, "Dmol3," *J. Chem. Phys.*, vol. 113, p. 7756, 2000, [Online]. Available: <https://www.3ds.com/fileadmin/PRODUCTS-SERVICES/BIOVIA/PDF/biovia-material-studio-dmol3.pdf>
- [34]. A. D. Becke and A. D. Becke, "Densityfunctional thermochemistry . III . The role of exact exchange Density-functional thermochemistry . III . The role of exact exchange," *J. Chem. Phys.*, vol. 5648, 1993, doi: 10.1063/1.464913.
- [35]. C. Lee, W. Yang, and R. G. Parr, "Development of the Colle-Salvetti correlation-energy formula into a functional of the electron density," *Phys. Rev. B*, vol. 37, 1988.
- [36]. S. H. Vosko, L. Wilk, and M. Nusair, "Accurate spin-dependent electron liquid correlation energies for local spin density calculations: a critical analysis," *Can. J. Phys.*, vol. 58, no. 8, pp. 1200–1211, 1980, doi: 10.1139/p80-159.
- [37]. T. A. Halgren and W. N. Lipscomb, "The synchronous-transit method for determining reaction pathways and locating molecular transition states," *Chem. Phys. Lett.*, vol. 49, no. 2, pp. 225–232, 1977, doi: 10.1016/0009-2614(77)80574-5.
- [38]. A. Fielicke, P. Gruene, G. Meijer, and D. M. Rayner, "The adsorption of CO on transition metal clusters: A case study of cluster surface chemistry," *Surf. Sci.*, vol. 603, no. 10–12, pp. 1427–1433, 2009, doi: 10.1016/j.susc.2008.09.064.
- [39]. A. Chiorino, E. Garrone, G. Ghiotti, E. Guglielminotti, and A. Zecchina, "Infrared study of Co Adsorption on extremely small metal clusters obtained by reduction under mild conditions of NiO-MgO and CoO-MgO solid solutions," *Stud. Surf. Sci. Catal.*, vol. 7, no. 1, pp. 136–148, 1981, doi: 10.1016/S0167-2991(09)60266-4.
- [40]. B. H. Morrow, D. E. Resasco, A. Striolo, and M. B. Nardelli, "CO adsorption on noble metal clusters: Local environment effects," *J. Phys. Chem. C*, vol. 115, no. 13, pp. 5637–5647, 2011, doi: 10.1021/jp108763f.